Malaysian Journal of Analytical Sciences (MJAS)





PERFORMANCE OF CERAMIC MEMBRANE COATED WITH GRAPHENE OXIDE AS ALTERNATIVE FOR OILY WASTEWATER TREATMENT

(Prestasi Selaput Seramik Grafin Oksida Sebagai Pilihan Untuk Rawatan Air Sisa Berminyak)

Nurdiyana Nabilah Kasim¹, Sharifah Abdullah¹, Nur Asmaliza Mohd Noor²

¹Faculty of Civil Engineering, Universiti Teknologi MARA, 40450 Shah Alam, Selangor, Malaysia ²Faculty of Civil Engineering, Universiti Teknologi MARA Pahang, Lintasan Semarak 26400 Jengka, Pahang, Malaysia

*Corresponding author: nurasmaliza@uitm.edu.my

Received: 20 November 2019; Accepted: 5 April 2020; Published: June 2020

Abstract

The high demand for liquefied natural gas (LNG) contributes to the increasing production of LNG thus leading to the increment of oily wastewater. The membrane technology shows a very promising alternative to replace the conventional method to treat oily wastewater. The objectives of this study are to synthesize graphene oxide (GO) as a modifier to graphitic carbon nitride (g- G_3N_4) for alumina ceramic membrane, to characterize the structure of nanosheet and bulk of graphitic carbon nitride, graphene oxide and g- G_3N_4 /GO composite which leads to the study of the performance of g- G_3N_4 /GO coated alumina ceramic photocatalytic membrane to degrade oil in oily wastewater. The methodology started with the material preparation, photocatalyse membrane preparation and the characterization of material using X-ray diffraction (XRD), Fourier Transformation Infrared (FTIR) analysis, Brunauer Emmet Teller (BET) surface area analyses and UV-Vis-NIR spectrophotometer analysis. The last method is the degradation of methylene blue (MB) dye and photocatalytic study degradation of oil in wastewater using synthesis oily wastewater. The results indicated the g- G_3N_4 /GO reduced 73.79% of the MB dye compared to 38.85% and 62.71% for bulk g- G_3N_4 and g- G_3N_4 nanosheet respectively. The g- G_3N_4 /GO composite photocatalyst showed remarkable photocatalytic efficiency rather than bulk g- G_3N_4 and g- G_3N_4 nanosheet. Thus, the introduction of GO into g- G_3N_4 has improved the charge separation efficiency of g- G_3N_4 and improving the organic degradation potential of g- G_3N_4 .

Keywords: alumina, g-C₃N₄, graphene oxide, photocatalytic membrane, wastewater oily

Abstrak

Permintaan yang tinggi terhadap gas asli cecair (LNG) menyumbang kepada peningkatan pengeluaran LNG sehingga mengakibatkan pertambahan terhadap air sisa berminyak. Teknologi selaput menjadi pilihan yang menggantikan kaedah konvensional dalam merawat air sisa berminyak. Objektif kajian ini adalah untuk melakukan sintesis grafin oksida (GO) sebagai pengubahsuai karbon nitrida grafit (g-C₃N₄), untuk memperincikan struktur lapisan nano, karbon nitrida grafit, grafin oksida dan g-C₃N₄/GO komposit yang membawa kepada kajian prestasi selaput fotomangkin seramik alumina bersalut g-C₃N₄/GO untuk degradasi minyak dalam air sisa berminyak. Kaedah kajian bermula dengan penyediaan bahan, penyediaan selaput fotomangkin dan pencirian bahan menggunakan pembelauan sinar-X (XRD), analisis inframerah trasnformasi Fourier (FTIR), analisis kawasan permukaan Brunauer Emmet Teller (BET) dan analisis spektrofotometer UV-Vis-NIR. Kaedah terakhir adalah degradasi pewarna metilena biru (MB) dan kaedah fotomangkin dalam degradasi minyak dalam air sisa menggunakan jenis

Nurdiyana Nabilah et al: PERFORMANCE OF CERAMIC MEMBRANE COATED WITH GRAPHENE OXIDE AS ALTERNATIVE FOR OILY WASTEWATER TREATMENT

tiruan. Keputusan kajian ini telah menunjukkan bahawa g- C_3N_4 /GO berkurang kepada 73.79% daripada pewarna MB berbanding 38.85% untuk g- C_3N_4 dan 62.71% untuk g- C_3N_4 lapisan nano. Manakala kaedah fotomangkin bagi komposit g- C_3N_4 /GO menunjukkan kecekapan fotomangkin yang luar biasa berbanding g- C_3N_4 dan g- C_3N_4 lapisan nano. Oleh itu, pengenalan GO ke dalam g- C_3N_4 telah meningkatkan kecekapan g- C_3N_4 sebagai agen pemisahan sekali gus meningkatkan potensi g- C_3N_4 sebagai degradasi organik.

Kata kunci: alumina, g-C₃N₄, grafin oksida, fotokatalik, selaput, air sisa berminyak

Introduction

Numerous processes and activities in various industries that have led to the production of wastewater are food processing, textile and oil and gas. In Malaysia, oil and gas industries are the major contribution in economy and thus a lot of activities related to these industries and causing major contribution to the production of wastewater. There are a few activities in oil and gas that produces was tewater such as raw natural gas that is fed into gas treating facilities such as acid gas removal unit (AGRU), mercury removal unit, and dehydration unit and then passed into the liquefaction unit to convert it into LNG. These units' associated facility leads to the generation of wastewater which can be divided into the conventional and non-conventional pollutants. The types of conventional pollutants which are also known as oily wastewater are oil and grease and suspended solids while the non-conventional pollutants which are known as chemically contaminated wastewater are phenolic compounds, sulphide and ammonia [1]. In this study, oily wastewater is emphasized due to the increase of its group therefore the proper and better oily wastewater treatment technology or strategies are needed to tackle these is sues. It is necessary to purify the wastewater in order to meet the environment's discharge standards by the Department of Environment (DOE) Malaysia because oily wastewater can cause adverse effects to the environment especially marine life as shown in Table 1 [2].

New technology has been introduced to treat oily wastewater using the membrane [3] where it has a function to act as a selective barrier to separate the pollutants from water. Previously, most of the studies have been conducted to improve the efficiency of alumina ceramic membrane to separate and treat wastewater. However recently, the addition of the degradation capability to facilitate the membrane separation process using photocatalyst such as carbon nitride, g-C₃N₄ on the surface of the ceramic membrane as quite a promising method has been introduced. Despite the fact that the membrane presents great potential to be applied in the separating process, yet it has fouling problems [4]. The fouling is hard to be removed and it could weaken the permeation rate through the membrane and affect the quality of treated wastewater [3]. Thus, the introduction of photocataly st on the surface of the membrane could contribute antifouling functions under light irradiation, sustain the clean membrane surface and improve the quality of treated wastewater. Therefore, the objectives of this study are to synthesize graphene oxide (GO) as a modifier to graphitic carbon nitride (g-C₂N₄) for alumina ceramic membrane, to characterize the structure of nanosheet and the bulk of graphitic carbon nitride, graphene oxide and g-C₃N₄/GO composite and to study the performance of g- C_3N_4 /GO coated alumina ceramic photocatalytic membrane to degrade oil in oily wastewater.

Table 1. Discharge of industrial effluent or mixed effluent of standard A and B [2]

Parameter	Unit	Standard A	Standard B
Temperature	0 C	40	40
pH Value	-	6.0-9.0	5.5-9.0
BOD ₅ at 20 ^o C	mg/L	20	50
Suspended Solid	mg/L	50	100
Mercury	mg/L	0.005	0.05
Cadmium	mg/L	0.01	0.02
Chromium Hexavalent	mg/L	0.05	0.05
Chromium Trivalent	mg/L	0.20	1.0
Arsenic	mg/L	0.05	0.10
Cyanide	mg/L	0.05	0.10
Lead	mg/L	0.10	0.50
Copper	mg/l	0.20	1.00
Manganese	mg/L	0.20	1.00
Nickel	mg/L	0.20	1.00
Tin	mg/L	0.20	1.00
Zinc	mg/L	2.00	2.00
Boron	mg/L	1.00	4.00
Iron (Fe)	mg/L	1.00	5.00
Silver	mg/L	0.10	1.00
Aluminum	mg/L	10	15.0
Selenium	mg/L	0.02	0.50
Barium	mg/L	1.0	2.00
Fluoride	mg/L	2.0	5.00
Formaldehyde	mg/L	1.0	2.00
Phenol	mg/L	0.001	1.00
Free Chlorine	mg/L	1.0	2.00
Sulphide	mg/L	0.05	0.05
Oil and Grease	mg/L	1.0	10
Ammoniacal Nitrogen	mg/L	10	20
Color	ADMI	100	200

Materials and Methods

To achieve the objectives of this study, the methodology can be divided into 4 Parts. Part 1 covers the material preparation, that is, synthesis of bulk graphitic carbon nitride synthesis of bulk graphitic carbon nitrite (g-C₃N₄) nanosheet and synthesis of GO. Part 2 involves the photocatalyst membrane preparation, that is, synthesis alumina ceramic, disc membrane, preparation of ceramic dope solution, fabrication of alumina ceramic disc membrane and synthesis of g-C₃N₄/GO alumina ceramic membrane. The work on material characterization of materials is done in Part 3 utilizing analyzes via XRD, FTIR, BET and UV-Vis-NIR. The last part which is Part 4 involves related pre photocatalysis studies such as degradation measurement of methylene blue (MB) dye and photocatalytic studies on the degradation of oil in wastewater using synthetic oily wastewater. Details of each above-mentioned methodology parts are discussed as follows:

Material preparation

The facile temperature free method was used for preparation of g- C_3N_4 by using urea powder (HmbG Chemical Germany) and isopropanol alcohol (IPA, 99.7%, M = 60.10 g/mol) bought from Hypercube IT Solution as dispersion medium to exfoliate the bulk g- C_3N_4 into gC_3N_4 nanosheet. GO was prepared by Hummers' method by using graphite powder (Comak) and sodium nitrate (Systerm, NaNO₃, ChemAR). Sonochemical method was used to prepare gC_3N_4 /GO composite.

Synthesis of bulk graphitic carbon nitride

The synthesis of bulk graphitic carbon nitride is achieved using the urea powder by applying facile template-free method [6]. An amount 20 g of urea powder purchased from HmbG Chemical was settled in a lidded alumina crucible and heated for 550 °C in a carbolite furnace for 4 hours using the heating rate of 15 °C/min.

Synthesis of bulk g-C₃N₄ nanosheet

Nanosheet form of $g-C_3N_4$ was synthesized using the liquid exfoliation method of $g-C_3N_4$ [7] in order to

have improved photocatalytic effect. This method used organic solvent isopropanol alcohol (IPA, 99.7%, M=60.10~g/mol) brought from Hypercube IT Solution as a dispersion medium where 0.3 g of bulk graphitic carbon nitride was dispersed into 100 mL of isopropanol alcohol. The dispersion was sonicated in room temperature for 8 hours to exfoliate the bulk g-CN then centrifuged at 3000 rpm for 30 minutes in order to give the homogenous dispersion of exfoliated g-C₃N₄ nanosheet. After that, the dispersion was dried at 50 °C for 6 hours in order to form and collect the final product which was a light-yellow powder of g-C₃N₄ nanosheet.

Synthesis of GO

GO was synthesized using the Hummers' method [8] where 5 g of graphite powder and 2.5 g of sodium nitrate was put in 1000 mL of concentrated sulphuric acid (H₂SO₄). Subsequently, the mixture was stirred for 1 hour and kept under low temperature by placing it in ice. After that, the 30 g of KMnO₄ was gradually added for 2 hours and continuously stirred for another 2 hours in room temperature and then heated with a temperature of 70 °C. Next, the 100 mL of water was gradually added to the mixture and stirred for another 1 hour. The $30\,\text{mL}$ of H_2O_2 was added into the mixture to stop the reaction and the color of the suspension turned to bright yellow. In order to purify the suspension, 0.2M of HCI was added once and the 200 mL of distilled water, 3 times until pH 7 (neutral). Then the sample was dried in the furnace with a temperature of 80 °C for a day in order to form GO.

Synthesis of g-C₃N₄/GO composite photocatalyst

The synthesis followed the sonochemical method ([9]) where 0.2 g of GO of previous synthesis was added into 200 mL of high purity water, 0.2g of g-C₃N₄ nanosheet was added into the mixture, sonicated for 12 hours, furnace dried in a temperature of 80 $^{\circ}$ C for a day.

Photocatalyst membrane preparation

This part started with the synthesis of alumina ceramic disc membrane as it was used as the base membrane in

this study. The other steps for preparation for photocatalyst membrane are as follows:

Preparation of ceramic dope solution

The ceramic dope solution was prepared first for the process fabrication of the ceramic membrane. It consisted of the composition of ceramic particle, a polymeric binder, solvent, additive that acts as the dispersant [10]. The ceramic particle was used as Al_2O_3 , alpha; 99.9% metal basis, surface area 6-8 m²/g, <1.0-micron APS powder, Alfa Aes ar for this research. Meanwhile dimethyl sulfoxide (HPLC grade, VWR), and polymeric binder polyethersulfone (PESf, Ameco Performance, USA) were used. Arlacel P135 (polyethylene glycol 30-dipolyhydroxystearate, Uniqema) was used as the additive. The process of preparation started with 55 wt.% of aluminum oxide powder, 0.38 wt.% of Arlacel weighed and added into 39.12 wt.% of the solvent, DMSO. Additionally, the mixture was rolled/milled with grinding balls for 48 hours. The ceramic dope solution was ready to be used to fabricate the ceramic disc membrane after adding 5.5 wt.% of PESf into the mixture and rolled for another 48 hours.

Fabrication of alumina ceramic disc membrane

The ceramic dope solution went through the inversion method where it needs to be poured into a stainless-steel mold with a diameter of 3 cm and placed in a water bath for 30 minutes and after it hardens, the precursor ceramic disk was removed. The next process was sintering the precursor ceramic disc calcite by using furnace CARBOLITE to obtain the final ceramic disc membrane. The temperature of the furnace was set at 600 °C at a rate of 2 °C/minute with a dwell time of 2 hours and has been increased to the targeted temperature of 1400 °C at a rate of 5 °C/minute with a dwell time of 4 hours. Then, the temperature was reduced to room temperature at a rate of 5 °C/minute and the alumina ceramic membrane was ready to be coated with the composite photocatalyst.

Synthesis of $g-C_3N_4/GO$ alumina ceramic membrane

The 0.3 g of g-C₃N₄/GO composite was dissolved in 50 mL of distilled water and sonicated for 1 hour. Then, g-

 C_3N_4 /GO solution was coated with alumina ceramic membrane by pouring the solution on the ceramic membrane surface and dried in the furnace at 50 $^{\circ}$ C for a day.

Characterization of material

Characterization of material for synthesized GO, bulk and nanosheet g-C₃N₄ and g-C₃N₄/GO composites used the XRD method which operated with 40 kV and 40 mA and the scanning rate was 2°/minute. Besides, the FTIR was also used to characterize the material with the operation of wavelength around 800-3800 cm⁻¹. Other methods that used to characterize material was BET Surface Area Analysis where the specific surface area and pore size distribution of synthesized materials in powder was determined by the adsorption of nitrogen gas on the surface of the solid powder by calculating the amount of adsorbate gas on the layer of surface. It was done by using 3-Flex Micromeritics system. As for determination of degradation rate of MB dye and oily wastewater, the UV-Vis- NIR spectrophotometer (Perkin Elmer, LAMBDA 750) was used to obtain spectra.

Photocatalytic study: Degradation of MB dye

The preliminary photodegradation study was conducted on MB dye by using bulk g-C₃N₄, g-C₃N₄ nanosheet, and g-C₃N₄/GO composite powder under sunlight. An amount 0.1 g of each material added into a beaker that contained 50 mL of 25 mb/L MB dye. Then the solution was placed under sunlight for 2 hours and for every 30 minutes, 3 mL of solutions was extracted using a syringe and this was used to analyze and determine the degradation efficiency by using the UV-Vis-NIR Spectrophotometer at λ > 400 nm.

Photocatalytic study: Degradation of oil in wastewater

Photodegradation study on synthetic oily wastewater was conducted by using g-C₃N₄/GO composite powder. The synthetic oily wastewater was prepared by mixing 1 L of distilled water and of 1mL West Lutong light crude oil (SG 0.84, API 37.7) in room temperature but under sunlight. Then, an amount 0.1g of g-C₃N₄/GO composite was added into a beaker which contained 50 mL oily wastewater. The solutions were needed to be

placed under sunlight for 2 hours, 3 mL of solution was extracted using a syringe for every 30 minutes to determine the degradation efficiency using UV-Vis-NIR spectrophotometer.

Results and Discussion

Characterization of material: XRD analysis

Figure 1 shows the XRD pattern of fabricated bulk g-C₃N₄ and g-C₃N₄ nanosheet. Two peaks were identified for both g-C₃N₄ where for bulk g-C₃N₄, dominant (002) diffraction peak was identified at $2\theta = 27.2^{\circ}$. It was indicated in the interlayer stacking of conjugated aromatic CN unit with $d = 3.27 \mu m$. The improvement of (002) peak's intensity was found in g-C₃N₄ nanosheet due to the enhancement in crystallinity of g-C₃N₄ after liquid exfoliation [11]. The small degree of shifting in (002) diffraction peak's point was identified from 27.2° in bulk g-C₃N₄ to 27.4° in g-C₃N₄ nanosheet. The same goes to the stacking distance from $d=3.27\mu m$ in bulk g-C₃N₄ to $d=3.25 \mu m$. Both bulk g-C₃N₄ and g- C₃N₄ nanosheet indicated minor (100) diffraction peak around 13.0° which corresponds to the in-plane structural packing of triazine units while the distance between pores of nitride in g-C₃N₄ are specified with planar distance of $d = 6.79 \mu m$ for (100) diffraction peak. The diffraction peak at a lower angle of about 11.4° GO implies the introduction of oxygen containing functional group of GO [12,13].

The XRD patterns of fabricated g-C₃N₄ nanosheet, GO and g-C₃N₄/GO composite are shown in Figure 2. GO shows intense (001) diffraction peak at $2\square = 9.8^{\circ}$ which is typical for GO and the same pattern has been reported by Dutrow and Clark [11]. The factors that contributed to that pattern were the existence of oxygenated functional group and introduction of H₂O molecule. A study conducted by Olumurewa et al. [14] indicated that the introduction of diffraction peak at low angle furnace that the graphite was successfully oxidized to the GO. The XRD pattern for g-C₃N₄/GO composite showed the two diffraction peaks which was around 27.3° and this was quite similar with the XRD pattern of g-C₃N₄ (002) peak thus indicating that the composite contains g-C₃N₄. This was consistent with the findings by Alamet al. [15] that introduction of GO into the $g-C_3N_4$ did not affect the structure of $g-C_3N_4$. The introduction of GO has caused the intensity of (002) diffraction peak of g-C₃N₄/GO to decrease and this proved that g-C₃N₄/GO has less layers than g-C₃N₄ and this is parallel with the report by Dutrow and Clark [11]. Besides that, the modification of GO into g-C₃N₄ also caused the widening of (002) diffraction peak and this condition was explained by authors, where it is caused by the wavelike motion of the layer of g-C₃N₄/GO composite.

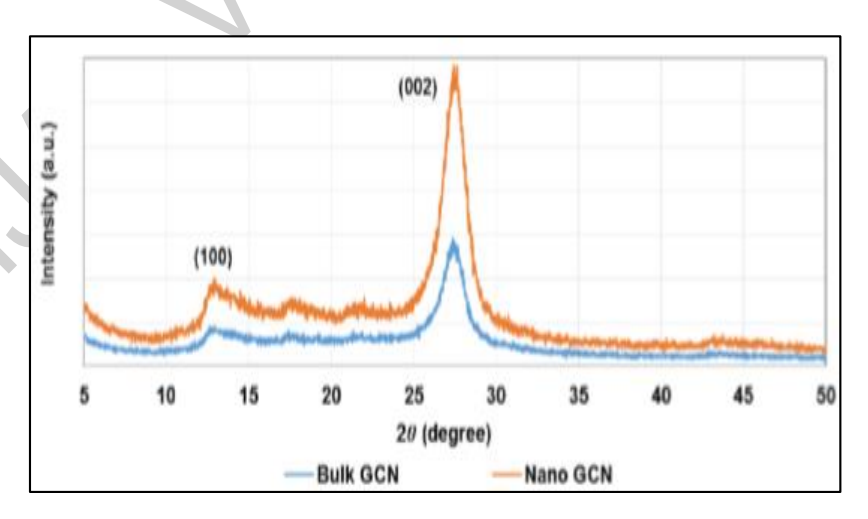


Figure 1. XRD pattern for bulk $g-C_3N_4$ and $g-C_3N_4$ nanosheet

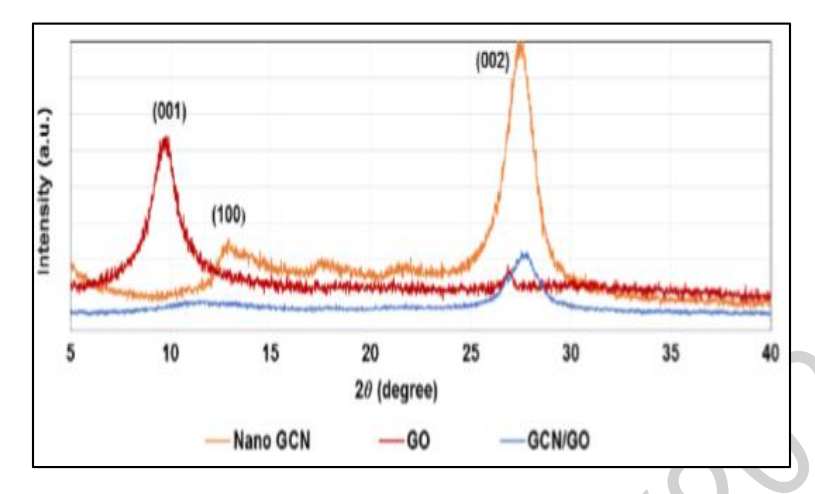


Figure 2. XRD patterns of g-C₃N₄ nanosheet, GO and g-C₃N₄/GO composite

FTIR analysis

Figure 3 shows FTIR spectrum of fabricated bulk g- C_3N_4 and g- C_3N_4 nanosheet with the wide absorption band at $3000-3400~\rm cm^{-1}$. According to Sheha [16], this is caused by the hydroxyl group due to the adsorption of H_2O molecule and uncondensed amine (-NH₂) or amine (-CH=NH). FTIR spectra of bulk g- C_3N_4 and g- C_3N_4 showed that at 1200 and 1220 cm⁻¹ respectively due to the characteristics of the breathing mode of heptazine ring system [17]. FTIR spectrum of bulk g- C_3N_4 and g- C_3N_4 nanosheet in Figure 3 are clearly identified and can be concluded that the exfoliation of g- C_3N_4 still retain their chemical structure as bulk g- C_3N_4 and this is aligned with the study conducted by Raphael [18].

The FTIR spectrum of g-C₃N₄/GO composite shows the resemblance pattern to the FTIR spectrum of g-C₃N₄ but with a slight difference to the GO as shown in Figure 4. The spectrum of GO shows the wider absorption band at a range of 3000-3500 cm⁻¹ attributed by the stretching of OH group of water molecules. Meanwhile, the g-C₃N₄/GO composite shows the same pattern of absorption band as GO and this is contributed by the stretching of N-H group. The g-C₃N₄/GO composite exhibited the sharp peak at 804.19 cm⁻¹ and the g-C₃N₄ nanosheet depicted the sharp peak at 1220 cm⁻¹. [19] conducted a study and found that the peak at 1039.31 cm⁻¹ caused by the presence of the C-

O functional group. Literature study [20] described that the peak at 1618.65 cm^{-1} was contributed by C=O stretching when at this stage the C=C bonds are still intact even after the oxidation process. Thus, this finding supports the justification for XRD analysis by introducing the GO into g- C_3N_4 and not altering the chemical structure of g- C_3N_4 .

BET analysis

Table 1 shows the value of surface area and pore volume of bulk $g-C_3N_4$, $g-C_3N_4$ nanosheet, $g-C_3N_4/GO$ composite and GO that was identified through the BET analysis.

The g-C₃N₄ nanosheet indicated the greater surface area and large pore volume compared to the other materials. The liquid exfoliation of bulk g-C₃N₄ has been minimized to the size of the nanometer thus the increase of specific areas for g-C₃N₄ was due to the bond cleavage of g-C₃N₄. BET surface area of g-C₃N₄ nanosheet was 94.08 m²/g greater than bulk g-C₃N₄ that was 79.84 m²/g as shown in Table 1. According to [21] the high surface area of g-C₃N₄ nanosheet would have the significant presence of active sites with nitrogen atomwhere it is very suitable to be used as a photocatalyst. Meanwhile, the BET surface area of GO and g-C₃N₄/GO composite were 2.01 m²/g and 45.57 m²/g respectively. These results have been agreed with the results produced by Vlachos et al. [22].

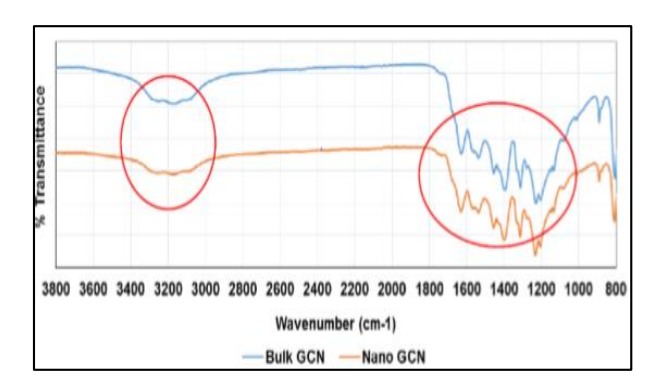


Figure 3. FTIR spectrum of bulk g-C₃N₄ and g-C₃N₄ nanosheet

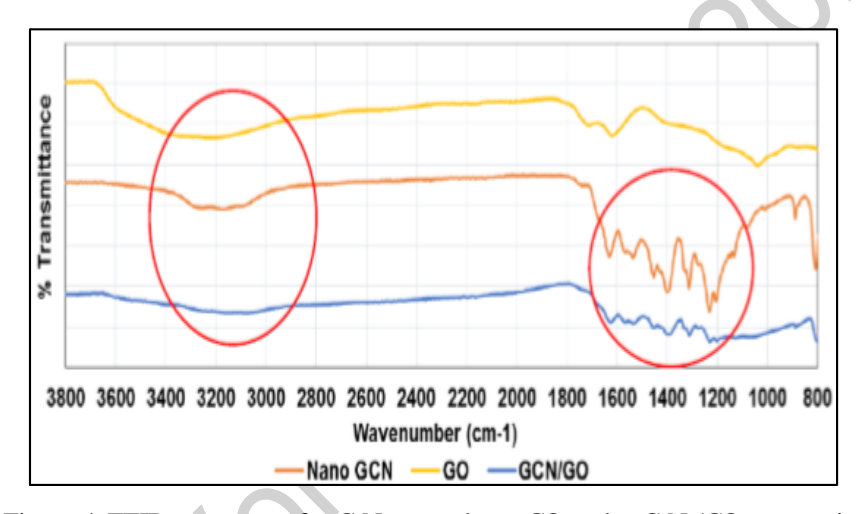


Figure 4. FTIR spectrum of g-C₃N₄ nanosheet, GO and g-C₃N₄/GO composite

Table 1. BET surface area and pore volume of material

Sample Name	Sample Mass (g)	SBET (m²/g)	Pore Volume (cm²/g)
Bulk g-C ₃ N ₄	0.086	79.840	0.465
g-C ₃ N ₄ nanosheet	0.048	94.079	0.639
g - C_3N_4/GO	0.224	45.572	0.057
GO	0.188	2.010	0.003

Photocatalytic study Degradation of MB dye

Photocatalysis is the method to measure the acceleration of chemical conversion through the activation of a catalyst. The preliminary photodegradation study under sunlight study was conducted on MB dye by using bulk g-C₃N₄, g-C₃N₄ nanosheet and g-C₃N₄/GO composite powder. Figure 5 shows the process of photocatalytic degradation of MB dye under sunlight for bulk g-C₃N₄, g-C₃N₄ nanosheet and g-C₃N₄/GO composite powder. The photocatalytic potential for different photocatalysts was evaluated by comparing the degradation efficiency for MB dye. The amount of MB dye degradation is 42.75% for g-C₃N₄/GO composite, 50.77% for g-C₃N₄ nanosheet and 31.29% for bulk g-C₃N₄ after 1 hour of exposure to sunlight can be seen through Figure 5. However, after 2 hours of exposure to sunlight, the amount of MB dye degradation has increased to 73.79% for g-C₃N₄/GO composite, 62.71% for g-C₃N₄ nanosheet and 38.85% for bulk g-C₃N₄. According to the findings, the bulk g-C₃N₄ and g-C₃N₄ nanosheet depicted the reduction of degradation efficiency after 30 minutes and 90 minutes of exposure to sunlight. However, the g-C₃N₄/GO composite indicated the consistency of the degradation efficiency throughout 2 hours of exposure. The g-C₃N₄ is to be the potential photocatalysts for the degradation of numerous pollutants with photophysical potential of the parent nitride altered through doping with heteroatoms, heterojunction formation with other materials and textural enhancements to expand the surface area and porosity [23].

Thus, the finding showed that the g- C_3N_4 /GO composite has a good degradation capability followed by g- C_3N_4 nanosheet and bulk g- C_3N_4 . The photocatalyst potential of g- C_3N_4 /GO composite was contributed by its characterization of chemical structure and properties. The introduction of GO has improved the charge of separation efficiency because when the visible light absorption capability g- C_3N_4 is combined with GO they act as electron sink [22] in helping the separation and storage to improve the photocatalytic capability of the composite. When g- C_3N_4 absorbed visible light, the electron is transferred to the GO layer where it reduces the chances of

electron-hole recombination thus improving the separation efficiency. However, the left holes on the valence band of g-C₃N₄ contributed to the consistent degradation efficiency of g-C₃N₄/GO composite. The factor that bulk g-C₃N₄ is having the lowest degradation efficiency compared to g-C₃N₄ nanosheet due to the low surface area where active site is less thus a low number of MB dye molecule is interacted with the photoexcited carrier [24]. As for g-C₃N₄ nanosheet, it slightly contradicts where it had a greater surface area thus greater availability of active sites to react with MB dye molecule.

Degradation of oil in wastewater

The potential of bulk g-C₃N₄, g-C₃N₄ nanosheet and g-C₃N₄/GO composite to degrade organic pollutants were tested with the evaluation of the efficiency of photocatalyst to degrade oil in synthetic oily wastewater under sunlight. Figure 6 shows the photocatalytic degradation of oil in synthetic oily wastewater under sunlight with bulk g-C₃N₄, g-C₃N₄ nanosheet and g-C₃N₄/GO composite powder. The g-C₃N₄/GO composite shows the consistent degradation efficiency after 1 hour with 49.65% of oil degraded while the bulk g-C₃N₄ only degraded to 35.24% of oil. After 2 hours, the results indicated that the amount of oil degraded was 75.54%, 55.89% and 44.57% for g-C₃N₄/GO composite, g-C₃N₄ nanosheet and bulk g- C_3N_4 respectively. The samples also produced initially, strong aromatic smells however, after 2 hours, the g-C₃N₄/GO composite produced a less aromatic smell. [25,26] also conducted a study using low cost ceramic membrane to treat synthetic oily wastewater and it showed a capability to treat oily wastewater.

Performance of G-C₃N₄/GO alumina ceramic membrane

Figure 7 shows the process of separation and photocatalytic degradation of oil in synthetic oily wastewater in bare alumina ceramic membrane and g- C_3N_4/GO alumina ceramic membrane. From the results obtained, the g- C_3N_4/GO alumina ceramic membrane showed a greater percentage of oil adsorption compared to the bare alumina ceramic membrane with 47.65% and 27.66% respectively after 2 hours. After the degradation and separation process, permeate water of g- C_3N_4/GO alumina ceramic membrane looked

clearer compared to the permeated water of bare alumina ceramic membrane according to the clarity of red scale. Moreover, there was no change in the intensity of aromatic smell of wastewater for both samples thus indicating that the aromatic compound is mostly not degraded. The coating of g-C₃N₄/GO on alumina ceramic membrane also had a greater removal efficiency of oil in oily wastewater rather than the bare

alumina ceramic membrane. This is due to the separation process of alumina ceramic membrane coupled with the degradation process of oil in the wastewater by gC_3N_4/GO [27]. In conclusion, $g-C_3N_4/GO$ alumina ceramic membrane can be a potential candidate to treat the industrial oily wastewater.

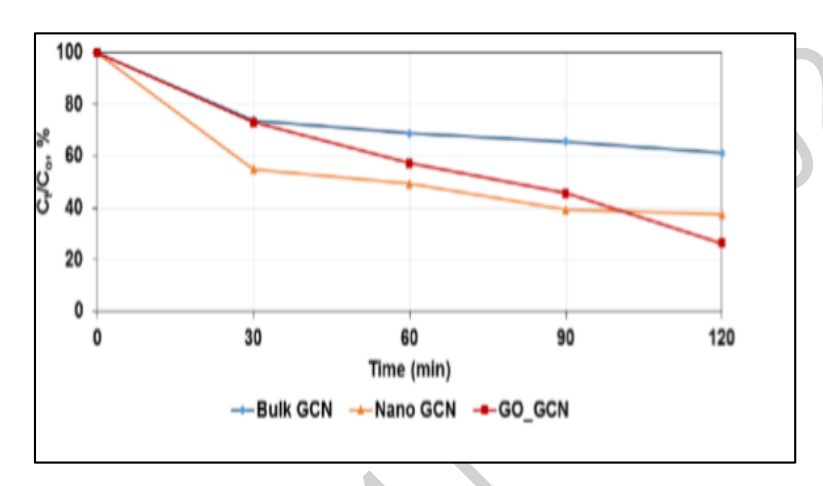


Figure 5. Photocatalytic degradation of MB dye under sunlight with bulk g- C_3N_4 , g- C_3N_4 nanosheet, and g- C_3N_4/GO composite

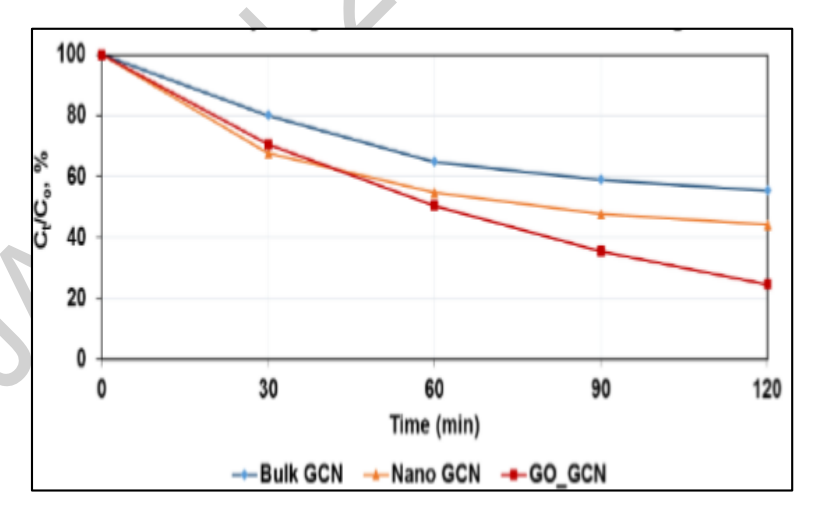


Figure 6. Photocatalytic degradation of oil in wastewater under sunlight with bulk g-C₃N₄, g-C₃N₄ nanosheet and g-C₃N₄/GO composite

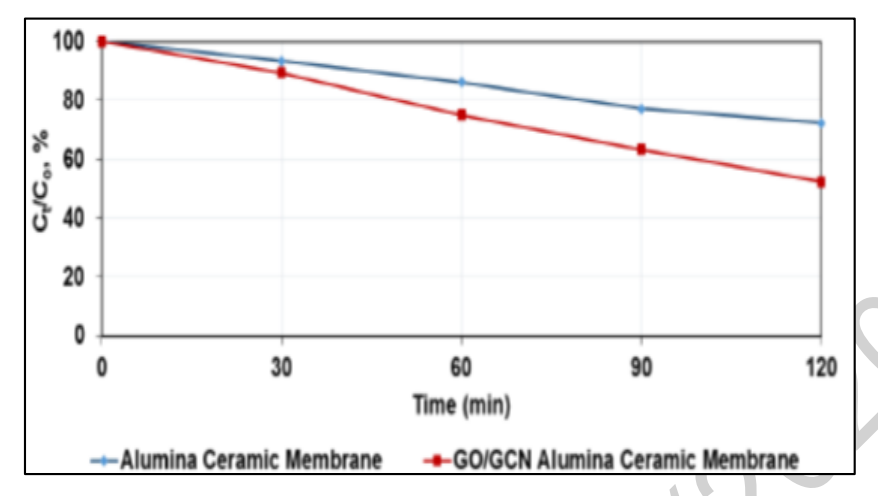


Figure 7. Separation and degradation of oil in synthetic oily wastewater with g-C₃N₄/GO alumina membrane and bare alumina membrane

Thus g- C_3N_4 /GO alumina ceramic membrane shows good removal capability of oil in oily wastewater when compared to bare alumina ceramic membrane. The improvement of the performance of alumina ceramic membrane to remove oil in the wastewater was contributed by the introduction of photocatalyst g- C_3N_4 /GO on the membrane surface. The additional g- C_3N_4 /GO photocatalyst opened up a new process that the degradation facilitates the removal of the organic compound of oil hence improving the quality of the permeated water

Conclusion

GO, photocatalyst bulk g- C_3N_4 , g- C_3N_4 nanosheet and g- C_3N_4 /GO composites were successfully synthesized and a major enhancement of photocatalytic potential under sunlight was achieved through the g- C_3N_4 /GO composite. According to the results of XRD analysis, bulk g- C_3N_4 and g- C_3N_4 nanosheet shows the dominant (002) diffraction peaks at $2\square = 27.2^0$ and $2\square = 27.4^0$ which validated that the materials prepared were correct. Besides, g- C_3N_4 shows improvement of (002) peak's intensity rather than bulk g- C_3N_4 due to the enhancement in crystallinity of g- C_3N_4 after liquid exfoliation. GO also successfully prepared and proved by results of XRD analysis where major (001) diffraction peak at $2\square = 9.8^0$. For FTIR analysis, a wide absorption band at 3000 - 4000 cm⁻¹ was

identified for both bulk g- C_3N_4 and g- C_3N_4 nanosheet where it was indicated that both had hydroxyl groups in the structure. Both photocatalysts also indicated an absorption band at $1203-1628~\rm cm^{-1}$ due to stretching of CN units in aromatic ring (RSC). FTIR spectrum of g- C_3N_4 /GO showed the wide absorption band at $3000-3400~\rm m^{-1}$ of FTIR spectrum which was close to the g- C_3N_4 which was attributed by stretching of the N-H group. This further strengthened the conclusion that introduction of GO into g- C_3N_4 did not alter the chemical structure of g- C_3N_4 .

The BET analysis showed that g-C₃N₄ nanosheet has a greater surface area than bulk g-C₃N₄ and g-C₃N₄/GO where the results are $94.08 \text{ m}^2/\text{g}$, $79.84 \text{ m}^2/\text{g}$ and 2.01 m^2/g respectively. The exfoliation of bulk g-C₃N₄ has minimized the size of the particle and improved the specific area of g-C₃N₄. This indicated that the exfoliation process was successful and the g-C₃N₄ bond was cleaved. The surface area of g-C₃N₄/GO was lower due to the stacking of layers on the structure of materials. The major enhancement of photocatalytic potential under sunlight was achieved by using g-C₃N₄/GO composite. The introduction of GO into g-C₃N₄ had improved the charge separation efficiency of g-C₃N₄ which enhanced the capability of g-C₃N₄ to MB and oil in oily wastewater. A g-C₃N₄/GO degraded 73.79% of MB dye rather than 38.85% and 62.71% for bulk g- C_3N_4 and g- C_3N_4 nanosheet. g- C_3N_4 /GO also degraded 75.54% of oil greater than bulk g- C_3N_4 and g- C_3N_4 nanosheet was 44.57% and 55.89% respectively. The exfoliation of g- C_3N_4 also showed a significant improvement in degradation capability of the g- C_3N_4 where, g- C_3N_4 nanosheet has a larger surface area with abundant active sites to react with photoexcited carriers compared to the bulk g- C_3N_4

References

- 1. Jacobs, D. (2011). The global market for liquefied natural gas. *Reserve Bank Australian Bulletin*, 9: 17-28.
- Department of Environment (2009). Discharge of industrial effluent or mixed effluent of standard A and B. Access from http://www.doe.gov.my/ eia/wp-content/uploads/2012/03/A-Guide-For-Investors 1.pdf. [Access online 20 March 2020].
- 3. Coca, J., Gutiérrez, G. and Benito, J. M. (2011). Treatment of oily wastewater. *NATO Science Peace and Security. Series C Environment Security*, 101: 1-55.
- 4. Won, W., Lee, S. K., Choi, K. and Kwon, Y. (2014). Current trends for the floating liquefied natural gas (FLNG) technologies. *Korean Journal of Chemical Engineering*, 31: 732-743.
- 5. De Angelis, L. and De Cortalezzi, M. M. F. (2013). Ceramic membrane filtration of organic compounds: Effect of concentration, pH, and mixtures interactions on fouling. *Separation and Purification Technology*, 118: 762-775.
- Goettmann, F., Thomas, A. and Antonietti, M. (2007). Metal-free activation of CO₂ by mesoporous graphitic carbon nitride. *Angewandte Chemie International Edition*, 46(15): 2717-2720.
- 7. Liu, J, Zhang, T., Wang, Z., Dawson, G. and Chen, W. (2011). Simple pyrolysis of urea into graphitic carbon nitride with recyclable adsorption and photocatalytic activity. *Journal of Materials Chemistry*, 21(38): 14398-14401.
- 8. Kang, J. H., Kim, T., Choi, J., Park, J., Kim, Y. S., Chang, M. S. and Park, C. R. (2016). Hidden second oxidation step of Hummers method. *Chemistry of Materials*, 28(3): 756-764.
- 9. Son, W.-J., Kim, J., Kim, J. and Ahn, W.-S.

- (2008). Sonochemical synthesis of MOF-5. *Chemical Communications*, 44(47): 6336-6338.
- Kang, J. S., Won, J., Park, H. C., Kim, U. Y., Kang, Y. S. and Lee, Y. M. (2000). Morphology control of asymmetric membranes by UV irradiation on polyimide dope solution. *Journal of Membrane Science*, 169(2): 229-235.
- 11. Dutrow, B. and Clark, C. (2015). X-ray powder diffraction (XRD), geochemical instrumentation and analysis. Access from http://serc.carleton.edu/research_education/geochemsheets/techniques/XR D.html [Accessed online: 20 March 2020].
- 12. Hummers, W. S. and Offeman, R. E. (1958). Preparation of oxide. *Journal of the American Chemical Society*, 80(6): 1339-1339.
- 13. Guo, L. P., Wang, J., Fu, F. and Wu, Z (2015). Three dimensional Fe3O4-graphene macroscopic composites for arsenate removal. Journal of Hazardous Materials, 298: 28-35.
- 14. Olumurewa, K. O., Olofinjana, B., Fasakin, O., Eleruja, M. A. and Ajayi E. O. B. (2017). Characterization of high yield graphene oxide synthesized by simplified Hummers method. *Graphene*, 6(4): 85-98.
- 15. Alam, S. N., Sharma, N. and Kumar, L. (2017). Synthesis of graphene oxide (GO) by modified Hummers method and its thermal reduction to obtain reduced graphene oxide (rGO). *Graphene*, 6(1): 1-18.
- 16. Sheha, E. (2014). Studies on TiO₂/reduced graphene oxide composites as cathode materials for magnesium-ion battery. *Graphene*, 3(3): 36-43.
- Bhargava, R., Wang, S. Q and Koenig, J. L. (2003). FTIR micro spectroscopy of polymeric systems. Advances in Polymer Science, 163: 137-191.
- 18. Raphael, L. (2011). Application of FTIR spectroscopy to agricultural soils analysis. *Fourier Transforms New Analytical Approaches FTIR Strategies*: pp. 385-404.
- 19. Gao, W. (2015). The chemistry of graphene oxide in Graphene oxide: Reduction recipes, spectroscopy and applications: pp. 61-95.
- 20. Yang, K., Peng, H., Wen, Y. and Li, N. (2010). Re-examination of characteristic FTIR spectrum of secondary layer in bilayer oleic acid-coated Fe₃O₄

- nanoparticles. *Applied Surface Science*, 256(10): 3093-3097.
- Vlachos, N., Skopelitis, Y., Psaroudaki, M., Konstantinidou, V., Chatzilazarou, A. and Tegou, E. (2006). Applications of Fourier transforminfrared spectroscopy to edible oils. *Analytica Chimica Acta*, 573: 459-465.
- 22. Gulmine, J.V., Janissek, P. R. Heise, H. M. and Akcelrud, L. (2002). Polyethylene characterization by FTIR. *Polymer Testing*, 21(5): 557563.
- 23. Darkwah, K. W. and Ao, Y. (2018). Mini review on structure and properties (photocatalysis) and preparation techniques of graphitic carbon nitride nano-based particles and its application. *Nanoscale Research Letter*, 13(388): 3-15.
- 24. Huh, Y. S. and Chang, Y. K. (2015). Selective silver ion adsorption onto mesoporous graphitic carbon nitride. *Carbon*, 95: 58-64.
- 25. Nandi, B. K., Das B., Uppaluri R., Purkait M. K.

- (2010). Studies on submicron range microfiltration inorganic membranes: Preparation characterization. *Membrane Water Treatment*, 1(2): 121-137.
- 26. Ranfang, Z., Gaoxiang, D., Weiwei, Z., Lianhua, L., Yanming, L., Lefu, M. and Zhoahui, L.(2014). Photocatalytic degradation of methane blue using TiO₂ impregnated diatomite. Advances in Materials Science and Engineering, 2014: 1-7.
- 27. Nguyen, H. T. V., Ngo, T. H. A., Do, K. D., Nguyen, M. N., To Dang, N. T., Nong Yuen, T. T. and Anh Vu, V. T (2019). Preparation and characterization of hydrophilic polysulfide membrane using graphene oxide. *Hindawi Journal of Chemistry*, 2019: 1-10.